Cell size distribution in random tessellations of space

Eloi Pineda*
Departament de Física i Enginyeria Nuclear, ESAB, Universitat Politècnica de Catalunya, Urgell 187, 08036 Barcelona, Spain

Pere Bruna and Daniel Crespo
Departament de Física Aplicada, EPSC, Universitat Politècnica de Catalunya, Avinguda del Canal Oímpic s/n, 08860 Castelldefels, Spain

(Received 10 May 2004; revised manuscript received 27 July 2004; published 10 December 2004)

Random subdivisions in a *D*-dimensional Euclidean space are commonly observed in many scientific fields, such as metallurgy, geology, biology, and even, in the case of large *D*, in subjects related to information codification. This paper presents an analytical approximation of the size probability distribution in space subdivisions generated by random point processes, which include the well-known cases of the Poisson-Voronoi and the Johnson-Mehl cellular structures. Based on the calculations of Gilbert [Ann. Math. Stat. **33**, 958 (1962)] and an assumption for the distribution shape, the cell size distributions are obtained in a general way for a very wide range of random space subdivisions.

DOI: 10.1103/PhysRevE.70.066119 PACS number(s): 02.50.Ey, 81.30.−t

I. INTRODUCTION

Random subdivisions of space can be obtained by many different processes. Specifically, the space subdivisions created during nucleation and growth processes are very important in many scientific fields, ranging from metallurgy and biology to ecology and social sciences [1]. This work addresses random tessellations formed when a certain medium is progressively occupied by growing domains appearing randomly in the untransformed space. The completely transformed medium becomes a cellular structure with properties depending on the nucleation frequency and the growth rate of the domains during the transformation. Among these kinds of cellular structures there are the well-known Poisson-Voronoi and Johnson-Mehl tessellations. However, an infinite number of different tessellations can be obtained by varying either the nucleation frequency or the growth rate.

Basing our calculations in those of previous papers, in Sec. II of this paper we will calculate an accurate approach to the cell size probability density function (PDF) of a Poisson-Voronoi tessellation in two- and three-dimensional spaces. These results will be generalized in Sec. III to compute the cell size PDF in the case of an arbitrary, time-dependent, nucleation frequency, with the Johnson-Mehl tessellation being the specific case of a constant nucleation frequency. As far as we know there is no similar approach in the literature. Finally, we will analyze the accuracy of our approach and we will discuss possible improvements.

II. CELL SIZE PROBABILITY DISTRIBUTION IN A POISSON-VORONOI TESSELLATION

The Voronoi network or tessellation is a well-known mathematical cellular structure and is widely applied in many diverse scientific fields [2–4]. This network divides the *D*-dimensional space into convex polyhedric cells, here called "crystals," and is built using an initial distribution of points, each one becoming a "seed" of one crystal. The face separating two neighboring polyhedra—of dimension $D-1$—bisects perpendicularly the line connecting their seeds. A random point seed distribution generates the well-known Poisson-Voronoi (PV) network; in this case the whole network is defined by a single parameter, namely, the density of seeds ρ. This PV tessellation has been widely studied in the literature; it is worth mentioning the works by Meijering [5] and Gilbert [6]. In these works several geometrical parameters of the PV tessellation were calculated using different techniques; among these, the Gilbert method for computing the variance of the crystal size distribution is particularly relevant to the present work. In the following, the size s will stand for the generalized *D*-dimensional volume of a cell.

Concerning the shape of the crystal size PDF, $f(s)$, an analytical result was derived only for the one-dimensional case [5,7], leading to

$$f(s) = 4s\rho^2 \exp(-2\rho s) \tag{1}$$

where s corresponds in this case to the crystal length. For higher dimensions only an empirical crystal size distribution has been proposed up to now; Kiang [2] and Weaire *et al.* [8] fitted a gamma distribution to the results of a computer simulated two-dimensional PV network. In this paper we will use this result, assuming that the crystal size PDF in a PV network is correctly described by the PDF of a gamma distribution, that is,

$$f(s) \propto s^{\nu-1} \exp(-\nu\rho s) \tag{2}$$

where the crystal size s would represent the crystal area and the crystal volume in the two- and three-dimensional cases, respectively. One can easily notice that this function matches the one-dimensional size PDF of Eq. (1) if $\nu=2$. Values of ν for higher dimensions were numerically fitted or analytically approximated [8,9].

*Electronic address: eloi.pineda@upc.es

A particularly interesting property of the gamma distribution is that the defining parameters ν and ρ can be expressed in terms of the expected value $E(s)$ and the variance var(s) as [10]

$$\rho = E(s)^{-1},$$

$$\nu = \frac{E(s)^2}{\mathrm{var}(s)}. \tag{3}$$

Hence, the results obtained by Gilbert [6] can be used to calculate the two-dimensional and three-dimensional size distributions. Some of these results will be recalled now to allow further development.

Gilbert studied the relation between the crystal size PDF, $f(s)$, and the probability density function that a random chosen point belongs to a crystal of size s. He found that this function is given by

$$f^*(s) = \frac{s}{E(s)} f(s), \tag{4}$$

which combines the fact that a large crystal has a proportionally large chance of containing the point, that is, $s/E(s)$, and the probability of finding such a crystal among the ensemble, which is given by $f(s)$. The expected size $E^*(s)$ of this new probability distribution is then

$$E^*(s) = \frac{E(s^2)}{E(s)}. \tag{5}$$

It follows that the knowledge of $E^*(s)$ would allow the determination of the variance var(s) and, consequently, of the exponent ν which determines the crystal size distribution.

Gilbert calculated $E^*(s)$ by means of a probability $P(b)$ that a randomly chosen point O and another point P at distance b are both contained in the same crystal. Such probability can be written as

$$P(b) = \rho \int \exp[-\rho V(Q,b)]\, dm(Q), \tag{6}$$

where $dm(Q)$ is the D-volume differential around a point Q, and then $\rho dm(Q)$ is the probability that a nucleation center is situated at point Q. The term $\exp[-\rho V(Q,b)]$ gives the probability that no other nucleation center is nearer to the points O and P, $V(Q,b)$ being the union of the two circular regions determined by points O, P, and Q sketched in Fig. 1. The integral is taken over all the points Q in the D-dimensional space.

In the specific cases of two and three dimensions the position of the point Q can be determined by the polar coordinates (r_O, θ_O) with respect to the point O, which implies $dm(Q) = 2 r_O dr_O d\theta_O$ $(D=2)$ and $dm(Q) = 2\pi r_O^2 \sin\theta_O dr_O d\theta_O$ $(D=3)$; thus r_O must be integrated from 0 to ∞ and θ_O from 0 to π. As shown in Fig. 1, the volume $V(Q,b) = V(r_O, \theta_O, b)$ can be expressed as

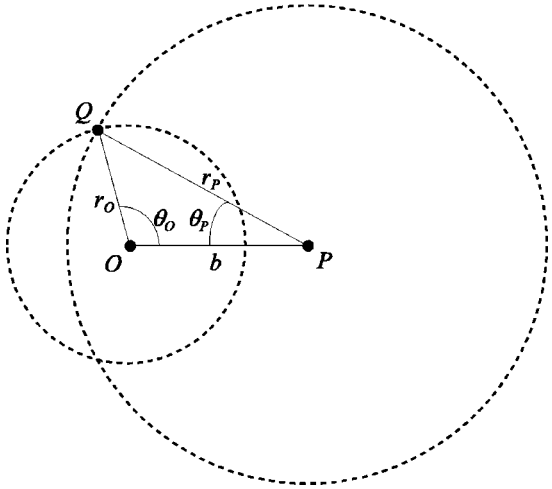

FIG. 1. Schematic drawing of the volume $V(Q,b)$ used in the calculation of probability $P(b)$.

$$V(r_O, \theta_O, b) = \begin{cases} \frac{1}{2}[r_O^2(\alpha_O - \sin\alpha_O) + r_P^2(\alpha_P - \sin\alpha_P)], & D=2, \\ \frac{\pi}{3}[h_O^2(3r_O - h_O) + h_P^2(3r_P - h_P)], & D=3, \end{cases} \tag{7}$$

where

$$\alpha_x = 2(\pi - \theta_x),$$

$$h_x = r_x(1 + \cos\theta_x), \tag{8}$$

and using the cosine theorem

$$r_p^2 = r_O^2 + b^2 - 2 r_O b \cos\theta_O,$$

$$\cos\theta_P = \frac{r_P^2 + b^2 - r_O^2}{2 r_P b}. \tag{9}$$

The expected value of the crystal size containing the random chosen point O, $E^*(s)$, can then be calculated as

$$E^*(s) = \frac{D\pi^{D/2}}{\Gamma(D/2+1)} \int_0^\infty P(b) b^{D-1} db \tag{10}$$

which is the integral over all the points P in the D-dimensional space weighted by its probability of belonging to the same crystal as point O.

The previous triple integral can be evaluated numerically; we used an extended midpoint algorithm [11] to an accuracy of 10^{-4}, obtaining $E^*(s) = 1.279\rho^{-1}$ and $1.179\rho^{-1}$ for two and three dimensions, respectively. Hence, applying Eqs. (3) and (5), it is obtained that

$$\nu = 3.575, \; D=2,$$

$$\nu = 5.586, \; D=3. \tag{11}$$

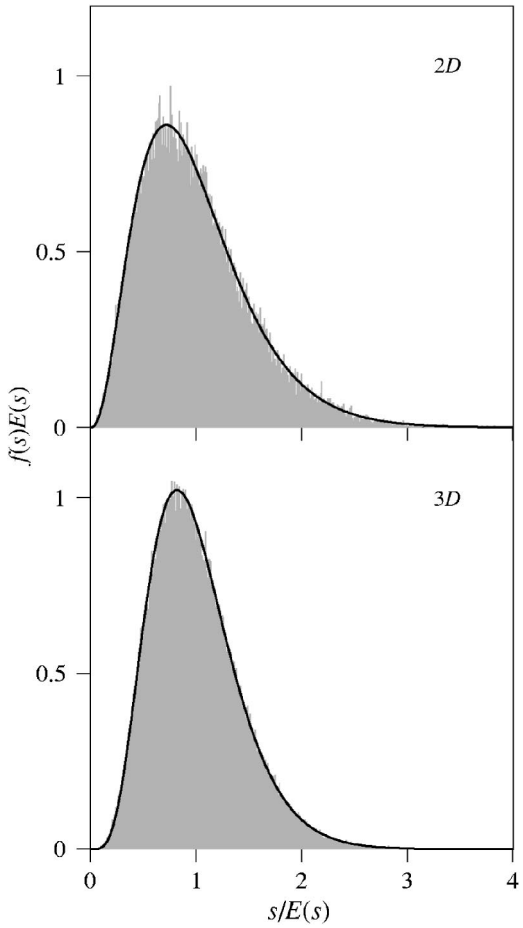

FIG. 2. Cell size probability density functions of PV tessellations in two and three dimensions. Comparison between stochastic simulations (grey bars) and a gamma distribution with the computed parameters (line).

It is worth saying that in the one-dimensional system, the integral of Eq. (10) can be analytically solved giving $E^*(s)=\frac{3}{2}\rho^{-1}$ and then $\nu=2$ as expected. In the case of higher dimensions, the validity of the gamma distribution assumption for a PV network can be checked against computer simulations of such systems. Figure 2 shows the comparison between the PDF of a gamma distribution, using the previous calculated variances, and the results of stochastic simulations. These simulations are performed in 2048×2048 and $256\times256\times256$ grids with periodic boundary conditions for the two- and three-dimensional PV tessellations, respectively. In these simulations the crystal seeds were randomly distributed and the seed density was chosen to ensure a number of crystals not less than 10^2; each grid point was afterward assigned to the crystal growing from the nearest seed. The results shown correspond to the average distribution obtained from 100 of such simulations in each case.

The results shown in Fig. 2 upheld the assumption of a gamma distribution for the crystal size distribution in a PV tessellation, as already shown in previous papers [2,8,9]. More important, the values of the variance and, consequently, the exponent ν determining this distribution can be calculated using the Gilbert method. This result is a useful tool for many scientific works where the PV network is employed; however, it has not been exploited in the literature, and costly stochastic simulations are usually performed when dealing with such systems.

III. CELL SIZE PROBABILITY DISTRIBUTION IN A TESSELLATION GENERATED BY AN ARBITRARY, TIME-DEPENDENT, RANDOM NUCLEATION

The PV tessellation is equivalent to the structure generated by a random distribution of crystal seeds, all growing at the same rate u and fixed in space without pushing apart as they grow into contact. Another important model of cellular structure, widely used in solid state transformations [12], is the one generated by crystal seeds appearing progressively as the time elapses. Each seed is then defined by a space position A_i and a "birth" time t_i, and the corresponding crystal is then made up by all the points such that the sphere growing at rate u from the seed (A_i,t_i) is the first to cover them. For the sake of simplicity, in this work we define a scaled birth time $\tau=ut$ which has length dimensions, a crystal seed being then determined by the (A_i,τ_i) position in a $(D+1)$-dimensional space.

When the seeds nucleated at each time τ constitute a random point distribution, the model is completely determined by a single function $\omega(\tau)$, the "nucleation" rate. This function is the density of seeds per unit volume attempting to appear in random spatial positions in the time interval $(\tau,\tau+d\tau)$, the seeds actually appearing only in the regions that are still not occupied by other crystals. In this paper we will refer to such cellular structure generating processes as "random nucleation models." The previously studied PV tessellation is a particular case of a random nucleation model with $\omega(\tau)=\rho\delta(\tau)$. Also the well-known Johnson-Mehl (JM) tessellation is obtained for $\omega(\tau)=\text{const}$; it is interesting to notice that in such a case the whole network is a semi-infinite, Poisson-Voronoi-like network in a $(D+1)$-dimensional space [6].

Several papers [4,13–16] studied the topological properties of such cellular structures. In the case of $D=1$ the crystal size distribution can be analytically derived by different techniques [5,7,17]. However, to our knowledge there is no theoretical approximation of the crystal size distribution generated in such models for $D>1$. Here, we will propose an approach to calculate this probability distribution. As a starting point, we will split the global crystal size PDF, $f(s)$, into τ functions $f_\tau(s)$ defined as the size probability density functions of the crystals with birth time τ.

The space fraction occupied at a certain time, $x(\tau)$, can be calculated by means of the so-called Avrami equation [18–22], which can be written as

$$x(\tau)=1-\exp\left(-\int_0^\tau \frac{\pi^{D/2}}{\Gamma(D/2+1)}(\tau-\tau')^D\omega(\tau')d\tau'\right). \tag{12}$$

The second term on the right hand side of this equation is the probability that a randomly chosen point is not occupied by

any τ' crystal at time τ, the term $[\pi^{D/2}/\Gamma(D/2+1)](\tau-\tau')^D$ being the volume of a D-dimensional sphere growing from a τ' seed. The validity of this equation has been extensively checked in the literature, and it has been obtained from purely statistical reasoning; see, for example, Ref. [23]. Using this Avrami equation, the number of τ seeds per unit volume actually nucleated can be easily calculated as

$$\rho_\tau d\tau = [1 - x(\tau)]\omega(\tau)d\tau, \tag{13}$$

which is the density of birth attempts multiplied by the remaining free space at time τ. Hence, the global size PDF can be written as

$$f(s) = \frac{\int_0^\infty \rho_\tau f_\tau(s) d\tau}{\int_0^\infty \rho_\tau d\tau} \tag{14}$$

in terms of the $f_\tau(s)$ functions.

In our approach we will consider that the τ seeds are distributed randomly inside the final space fraction occupied only by τ crystals; under this hypothesis, we can consider that the partitioning of this space will be similar to the one obtained in a PV tessellation, where the whole space is partitioned between randomly distributed seeds. Therefore, each $f_\tau(s)$ will be the PDF of a gamma distribution,

$$f_\tau(s) \propto s^{\nu_\tau - 1} \exp\left(\frac{-\nu_\tau s}{E_\tau(s)}\right), \tag{15}$$

determined by the expected value $E_\tau(s)$ and an exponent ν_τ. The validity and accuracy of this hypothesis will be discussed later in the paper by analyzing the obtained results. The $f_\tau(s)$ functions are determined if their expected value $E_\tau(s)$ and variance $\mathrm{var}_\tau(s)$ can be calculated, the exponent ν_τ being

$$\nu_\tau = \frac{E_\tau(s)^2}{\mathrm{var}_\tau(s)}. \tag{16}$$

$E_\tau(s)$ can be calculated in many different ways. Here we will calculate first the space fraction occupied only by τ crystals in the final tessellation, which is

$$x_\tau d\tau = \frac{D\pi^{D/2}}{\Gamma(D/2+1)}\omega(\tau)d\tau \int_0^\infty C_\tau(r) r^{D-1} dr, \tag{17}$$

where $\omega(\tau)d\tau$ is the density of possible τ seeds, $[D\pi^{D/2}/\Gamma(D/2+1)]r^{D-1}dr$ is the D-dimensional volume of a corona of radius r centered on a τ seed and

$$C_\tau(r) = \exp\left(-\int_0^{r+\tau} \frac{\pi^{D/2}}{\Gamma(D/2+1)}(r+\tau-\tau')^D \omega(\tau')d\tau'\right) \tag{18}$$

is the probability that a point P in this corona has no τ' seed closer than $r+\tau-\tau'$, which is the length grown by a τ' crystal in the same time the τ crystal has grown r. The upper limit of the integral is taken because a seed nucleated at a time $\tau' > r+\tau$ always finds any point of the corona already occupied. Figure 3 shows schematically the regions involved in such calculation. Using Eqs. (17) and (13), the expected value of a τ-crystal size is then easily obtained as

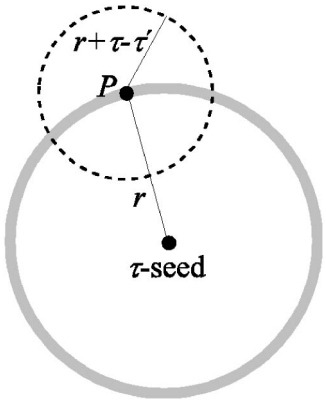

FIG. 3. Sketch of the regions involved in the calculation of x_τ.

$$E_\tau(s) = \frac{x_\tau}{\rho_\tau}, \tag{19}$$

that is, the space fraction occupied by τ crystals divided by the number of such crystals.

For the calculation of $\mathrm{var}_\tau(s)$ a Gilbert-like method will be adopted. While Gilbert calculated the variance of the global size distribution for the JM tessellation, here we will show that it is also possible to calculate the variance of the τ-crystal size distributions. Furthermore, here we will calculate such variances not only for the JM tessellation but for any random nucleation model determined by a nucleation rate $\omega(\tau)$.

Following the same reasoning as in the previous section, the variance will be now calculated by means of the probability density function $f_\tau^*(s)$ that a random chosen point belongs to a τ crystal of size s, which is

$$f_\tau^*(s) = x_\tau \frac{s}{E_\tau(s)} f_\tau(s) = \rho_\tau [s f_\tau(s)]. \tag{20}$$

Here, x_τ is the probability that a random point belongs to the space fraction occupied by τ crystals, $s/E_\tau(s)$, is the term stating that a large crystal has a proportionally large chance of containing the point, and $f_\tau(s)$ accounts for the probability of finding a crystal of such a size among the ensemble of τ crystals. From the previous equation one can easily obtain that

$$\mathrm{var}_\tau(s) = \frac{E_\tau^*(s)}{\rho_\tau} - [E_\tau(s)]^2 \tag{21}$$

and regarding Eq. (16)

$$\nu_\tau = \left(\frac{E_\tau^*(s)}{\rho_\tau [E_\tau(s)]^2} - 1\right)^{-1}. \tag{22}$$

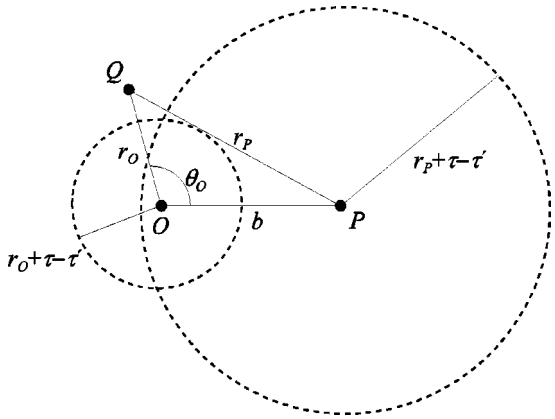

FIG. 4. Schematic drawing of the volume $V(Q,b,\tau-\tau')$ used in the calculation of probability $P_\tau(b)$.

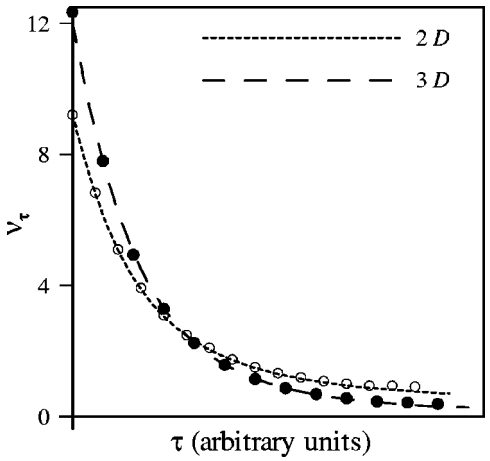

FIG. 5. v_τ parameters of the τ distributions computed with the analytical equations (lines) and obtained from stochastic simulations (symbols) for a Johnson-Mehl model in two and three dimensions.

As in the previous section, the calculation of $E_\tau^*(s)$ will be related to the probability $P_\tau(b)$ that two randomly chosen points O and P separated by a distance b belong to the same τ crystal, which can be written as

$$P_\tau(b) = \omega(\tau) \int \exp\left[- \int_0^\infty V(Q,b,\tau-\tau')\omega(\tau')d\tau' \right] dm(Q), \tag{23}$$

the integral taken over all the points Q of the D-dimensional space. The term $\omega(\tau)dm(Q)$ is the probability of a τ seed to be placed at point Q, and the exponential term is the probability that there is no other crystal which can occupy the points O and P before the crystal nucleated at Q.

In the case of two and three dimensions the point Q can be determined by the polar coordinates (r_O, θ_O) with respect to the point O, the D-dimensional volume $V(Q,b,\tau-\tau')$ being then calculable as the union of the two circular or spherical regions with centers at points O and P schematically depicted in Fig. 4. For the sake of simplicity, we will define the distance $d=\tau-\tau'$, which is the difference between the radius of two D-dimensional spheres growing from τ and τ' seeds. If two points O and P separated by a distance b belong to the same τ crystal with seed at position Q, any other τ' seed must be outside the spheres defined by the radii $r_{O,d}=r_O+d$ and $r_{P,d}=r_P+d$, where r_O and r_P are the distances from point Q to points O and P. When these two spheres overlap, which means $r_{O,d}+r_{P,d}>b$, their union can be written as

$$V(Q,b,d) = \begin{cases} \dfrac{1}{2}[r_{O,d}^2(\alpha_{O,d} - \sin\alpha_{O,d}) + r_{P,d}^2(\alpha_{P,d} - \sin\alpha_{P,d})], & D=2, \\ \dfrac{\pi}{3}[h_{O,d}^2(3r_{O,d} - h_{O,d}) + h_{P,d}^2(3r_{P,d} - h_{P,d})], & D=3, \end{cases} \tag{24}$$

where

$$\alpha_{x,d} = 2(\pi - \theta_{x,d}),$$

$$h_{x,d} = r_{x,d}(1+\cos\theta_{x,d}), \tag{25}$$

and

$$r_{P,d}^2 = r_{O,d}^2 + b^2 - 2r_{O,d}b\cos\theta_{O,d},$$

$$r_{O,d}^2 = r_{P,d}^2 + b^2 - 2r_{P,d}b\cos\theta_{P,d}. \tag{26}$$

If $r_{O,d}+r_{P,d}<b$, the two spherical regions become nonoverlapped and then $V(Q,b,d)$ is calculated as

$$V(Q,b,d) = \frac{\pi^{D/2}}{\Gamma(D/2+1)}[r_{O,d}^D + r_{P,d}^D]. \tag{27}$$

The above equations allow $V(Q,b,d)$ to be expressed in terms of $r_{O,d}$, $r_{P,d}$, b, and d. The basic relationship provided by the cosine theorem in Eq. (9) is still valid for obtaining $r_P=r_P(r_O,\theta_O,b)$ and using the definitions of $r_{O,d}$, $r_{P,d}$, and d one obtains $V=V(r_O,\theta_O,b,\tau-\tau')$. Given that $dm(Q)=2r_O dr_O d\theta_O$ $(D=2)$ and $dm(Q)=2\pi r_O^2\sin\theta_O dr_O d\theta_O$ $(D=3)$ the integrals in Eq. (23) become well defined for the two- and three-dimensional cases.

As in the previous section, the expected value $E_\tau^*(s)$ can be calculated by means of a D-dimensional spatial integral

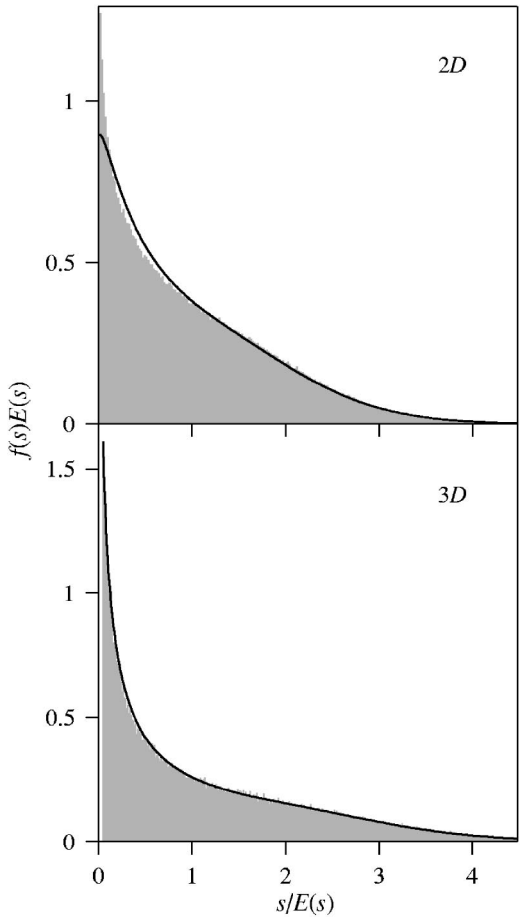

FIG. 6. Cell size probability density functions of JM tessellations in two and three dimensions. Comparison between stochastic simulations (grey bars) and a sum of gamma distributions with the computed parameters (line).

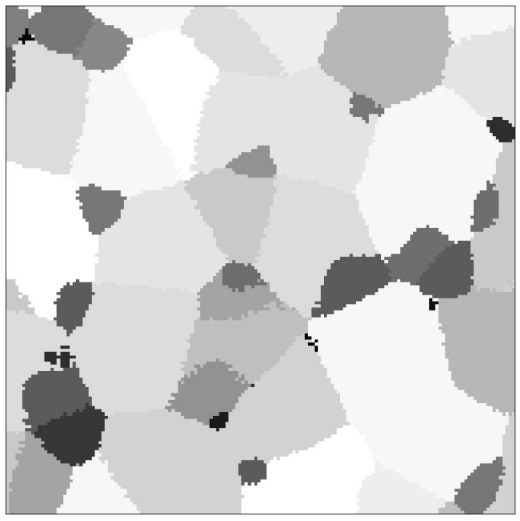

FIG. 7. Partial view of a stochastic simulation of a two-dimensional JM tessellation. Different grey intensities correspond to crystals with different birth times.

over all points P weighted by the probability $P_\tau(b)$ of belonging to the same crystal as point O, that is,

$$E_\tau^*(s) = \frac{D\pi^{D/2}}{\Gamma(D/2+1)} \int_0^\infty P_\tau(b) b^{D-1} db. \tag{28}$$

This multiple integral can be handled numerically for any nucleation rate function $\omega(\tau)$.

The results of the integrals in Eqs. (12), (17), and (28), jointly with Eq. (22), allow the calculation of the ν_τ exponent and then the obtainment of the τ distributions. Figure 5 (lines) shows the ν_τ values versus the birth time τ calculated

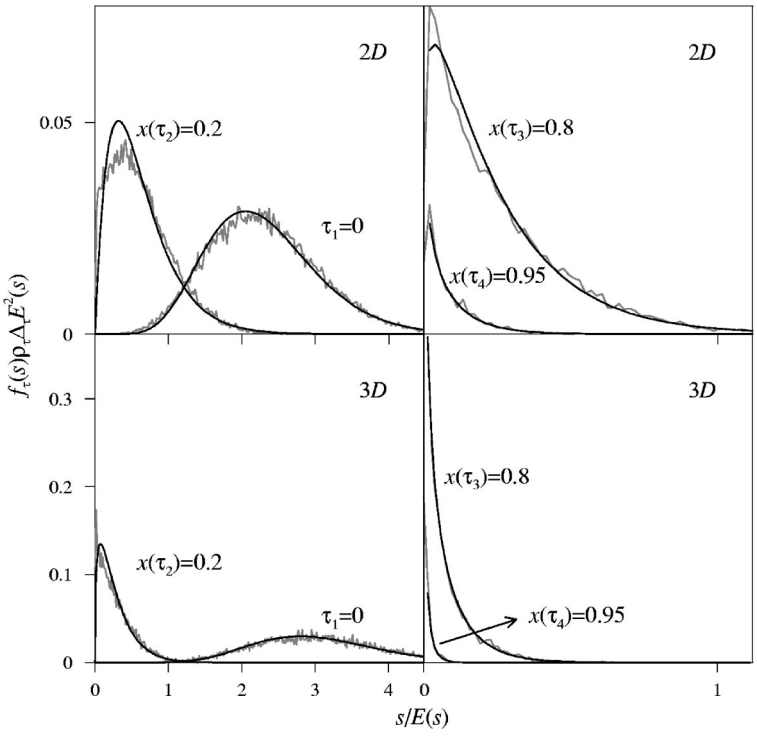

FIG. 8. Size probability density functions of crystals with a given birth time τ of a JM tessellation in two dimensions (top plots) and three dimensions (bottom plots). Comparison between stochastic simulations with time step Δ_τ (grey lines) and the computed functions assuming a gamma distribution (black lines).

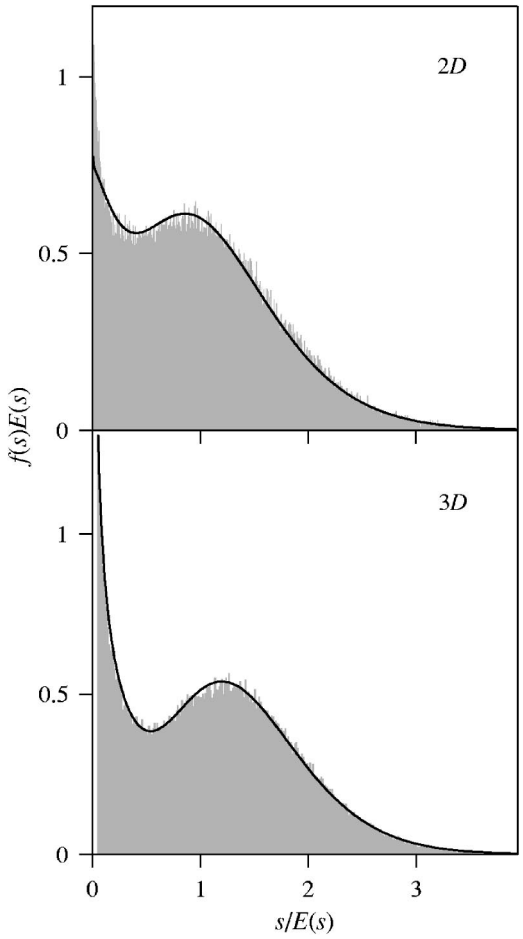

FIG. 9. Cell size probability density functions of tessellations obtained for a "preexisting + constant" nucleation law in two and three dimensions. Comparison between stochastic simulations (grey bars) and a sum of gamma distributions with the computed parameters (line).

for a JM model $[\omega(\tau)=\text{const}]$ to an accuracy of 10^{-3}. Regarding Eq. (16), these results imply that the relative dispersion of the $f_\tau(s)$ functions, $\text{var}_\tau(s)/E_\tau^2(s)$, increases with τ. As already stated in previous works, the growth of an "earlier" nucleated, and therefore probably large, crystal is little affected by impinging on a "later" nucleated, and therefore probably small, crystal. On the contrary, the growth of this small crystal is considerably affected by impinging on the neighboring large one. This means the final shapes of the crystals with the lowest nucleation time τ are expected to be much more homogenous than the ones with the highest τ, thus implying a lower dispersion around the expected value $E_\tau(s)$.

These analytical results were compared to stochastic simulations of two- and three-dimensional JM tessellations, and the ν_τ values obtained are also plotted in Fig. 5 (symbols). These stochastic simulations are performed using the same grids as for the PV tessellations shown in the previous section. In this case, the generation of the final tessellation is performed by time steps, each of them consisting of three substeps: (1) a new set of crystal seeds is randomly distributed with some fixed density; (2) a growth process increases the crystals' radii some fixed amount; (3) each grid point is ascribed to the crystal that reaches it first. The simulation executes time steps successively until the whole space is completely covered. As in the previous section, the results presented here are the averaged results of 100 simulations, and ν_τ is calculated through the statistical computation of the variance and the mean volume of the simulated crystals. It can be noted that the agreement between these stochastic simulations and the analytical computation is excellent.

Figure 6 shows the plot of the cell size PDF $f(s)$ obtained from Eqs. (14) and (15) against the results of the stochastic simulation of a JM tessellation. As observed in the figure, the cell size PDF obtained from the stochastic simulations is well reproduced by the procedure presented here; the agreement is excellent for $D=3$, while slight deviations can be noticed in the lowest cell values for $D=2$. As the computation of the variances is analytical, the source of this discrepancy is the assumption of a gamma probability distribution for the τ-crystal size.

It is worth noticing here that the assumption made in Eq. (15) is based on the empirical result obtained for the PV tessellation, where the size crystal distribution was well described by a gamma distribution. However, there exists a significant difference between the PV tessellation and a set of τ crystals in an arbitrary random nucleation model. Although the τ seeds are randomly distributed inside the space fraction $x_\tau d\tau$ occupied by the τ crystals, such space is not a continous space. Indeed, in the case of a JM tessellation there is a low probability of finding two neighbor crystals with the same birth time τ. Figure 7 shows a partial view of a simulated two-dimensional JM tessellation where the birth times of the crystals are shown as different gray intensities; the clearer the grain the lower its birth time. A detailed analysis of the tessellations obtained from stochastic simulations showed that there is a very low probability to find a pair of neighbor crystals nucleated at the same simulation time step.

From this discussion it follows that it is convenient to check the accuracy of the assumption made in Eq. (15). Figure 8 compares the proposed $f_\tau(s)$ functions to the size PDF obtained from simulations of two- and three-dimensional JM tessellations for crystals with four different birth times τ, namely, $\tau_1=0$, $x(\tau_2)=0.2$, $x(\tau_3)=0.8$, and $x(\tau_4)=0.95$. This allows us to analyze crystals born either at the initial on the final time steps of the simulations; note that the abscissa scale needs to be enlarged in the latter cases to show the features of the curve. Again, the shape of the simulated τ-crystal size PDF is close to that of a gamma distribution, although the agreement is not as good as for the PV tessellations discussed in the previous section. A deep analysis of the simulated $f_\tau(s)$ shows that they have systematically a kurtosis value lower than that of the corresponding gamma distribution.

Finally, with the aim of checking further the approximation presented in this paper, Fig. 9 shows the results obtained for a different random nucleation model. In this case the tessellation is generated by a nucleation law given by $\omega(\tau)=\rho_0\delta(\tau)+\omega_0$, that is, a certain amount of preexisting seeds followed by a constant nucleation. The values of ρ_0 and ω_0 are chosen to achieve a tessellation with exactly the same

quantity of preexisting and posteriorly nucleated crystals. This is indeed a combination of the nucleation laws leading to the already discussed PV and JM tessellations. As observed in Fig. 9, the model presented in this paper is also able to accurately describe the size distribution obtained for this nucleation law.

IV. CONCLUSIONS

This paper presents an approach to the computation of the cell size probability distribution in tessellations generated by random nucleation processes. The approach is an extension of the work of Gilbert [6], and it is based on the calculation of the means and variances of the τ distributions (size distributions of cells nucleated at a certain time τ) which made up the whole size distribution when integrated over all the nucleation times. A gamma probability distribution is assumed for the description of the τ distributions and their defining parameters are obtained through the computation of the corresponding distribution variances. The results obtained compare satisfactorily to stochastic simulations in the case of two- and three-dimensional JM tessellations. Slight deviations between the presented method and the stochastic simulations are attributed to the assumption of gammalike τ distributions. Further development of the present work could be quickly performed if a more accurate distribution shape was proposed for the τ distributions. In this sense, understanding why the PV tessellation is accurately predicted by a gamma distribution would be of maximum interest; unfortunately, this still remains an unsolved problem.

Despite the small deviations already discussed, the theory developed in this paper allows the calculation of the cell size probability distribution of tessellations generated in nucleation and growth systems with arbitrary, time-dependent, nucleation protocols. The application of this work is then very wide, involving obvious scientific fields, such as metallurgy, but also a wide range of sciences where nucleation and growth processes are commonly observed.

ACKNOWLEDGMENTS

This work was funded by CICYT, Grant No. MAT2001-0957, and Generalitat de Catalunya, Grant No. 2001SGR00190.

[1] D. Stoyan, W. S. Kendall, and J. Mecke, *Stochastic Geometry and Its Application* (Akademie-Verlag, Berlin, 1989), Chap. 10, p. 260.
[2] T. Kiang, Z. Astrophys. **64**, 433 (1966).
[3] J. L. Finney, J. Mol. Biol. **119**, 415 (1978).
[4] S. Kumar and S. K. Kurtz, Mater. Charact. **31**, 55 (1993).
[5] J. L. Meijering, Philips Res. Rep. **8**, 270 (1953).
[6] E. N. Gilbert, Ann. Math. Stat. **33**, 958 (1962).
[7] J. D. Axe and Y. Yamada, Phys. Rev. B **34**, 1599 (1986).
[8] D. Weaire, J. P. Kermode, and J. Weichert, Philos. Mag. B **53**, L101 (1986).
[9] P. N. Andrade and M. A. Fortes, Philos. Mag. B **58**, 671 (1988).
[10] Z. Fan, Y. Wu, X. Zhao, and Y. Lu, Comput. Mater. Sci. **29**, 301 (2004).
[11] W. H. Press, S. A. Teukolsky, W. T. Vetterling, and B. P. Flannery, *Numerical Recipes in Fortran: The Art of Scientific Computing* (Cambridge University Press, Cambridge, U.K., 1992), Chap. 4.
[12] A. Korobov, J. Math. Chem. **24**, 261 (1998).
[13] J. Moller, Adv. Appl. Probab. **24**, 814 (1992).
[14] P. A. Mulheran, Philos. Mag. Lett. **66**, 219 (1992).
[15] S. Kumar, S. K. Kurtz, J. R. Banavar, and M. G. Sharma, J. Stat. Phys. **67**, 523 (1992).
[16] T. Ohta, D. Jasnow, and K. Kawasaki, Phys. Rev. Lett. **49**, 1223 (1982).
[17] G. Yu, L. Deng, S. Yuan, and L. Zhang, Z. Metallkd. **87**, 508 (1996).
[18] M. Avrami, J. Chem. Phys. **7**, 1103 (1939).
[19] M. Avrami, J. Chem. Phys. **8**, 212 (1940).
[20] M. Avrami, J. Chem. Phys. **9**, 177 (1941).
[21] W. A. Johnson and P. A. Mehl, Trans. AIME **135**, 416 (1939).
[22] A. N. Kolmogorov, Izv. Akad. Nauk SSSR, Ser. Fiz. **3**, 355 (1937).
[23] G. Yu and J. K. L. Lai, J. Appl. Phys. **79**, 3504 (1996).